ORIGINAL PAPER

THE INHIBITORY ACTIVITY OF ALOISINES ON GSK-3β: STRUCTURE-ACTIVITY CORRELATION AND MOLECULAR DOCKING STUDIES

EMILIA AMZOIU[1], IONELA BELU[1], ADRIAN BETERINGHE[2*], MIHAELA SIMONA SUBTIRELU[1*], GEORGETA SOFIA POPESCU[3], MARIA VIORICA CIOCILTEU[1], DENISA CONSTATINA AMZOIU[1], GABRIELA RAU[1], OANA TAISESCU[4], MANUEL OVIDIU AMZOIU[1]

Manuscript received: 10.01.2026; Accepted paper: 12.03.2026; Published online: 30.03.2026.

Abstract. *Glycogen synthase kinase-3 is a fascinating enzyme involved in a series of physiological processes, and its activity is associated with the pathological features of various diseases, such as type 2 diabetes, Alzheimer's disease, chronic inflammation, cancer, and bipolar affective disorder. GSK-3 inhibitors are currently being tested for their therapeutic effects on these diseases. In this work, the inhibition of GSK-3β by aloisines is investigated by structure-activity correlation studies, the best model obtained being characterized by R^2 = 0.8865. The identification of the molecular fragments that contribute most to the formation of biological activity is carried out using fingerprint descriptors, such as the electronegativity of the OMO/UMO quantum molecular states. For an even better understanding of the relationship between chemical structure and observed biological activity, an aloisine/GSK-3β complex structure was obtained using molecular docking. The two types of studies (correlation and docking) are in good and complementary agreement. Therefore, our study suggests that the aloisine molecules are potent and selective for GSK-3β.*

Keywords: *aloisines; quantitative structure–activity relationship; molecular descriptors; glycogen synthase kinase-3β; molecular docking.*

1. INTRODUCTION

Glycogen synthase kinase-3 beta (GSK-3β) is a serine/threonine kinase that plays a crucial role in numerous cellular processes, including metabolism, cell proliferation, and apoptosis. Dysregulation of GSK-3β has been implicated in various pathological conditions, such as Alzheimer's disease, diabetes, and cancer, making it a significant target for therapeutic intervention. Aloisines, a group of natural compounds, have recently attracted attention for their potential inhibitory activity against GSK-3β.

The enzyme GSK-3 (Glycogen synthase kinase-3) is abundant in the brain and other tissues and is a key regulator of numerous signalling pathways [1,2].

[1] University of Medicine and Pharmacy, Faculty of Pharmacy, 200349 Craiova, Romania.
E-mail: emilia.amzoiu@umfcv.ro; ionela.belu@umfcv.ro; maria.ciocilteu@umfcv.ro; denisa.amzoiu@umfcv.ro; gabriela.rau@umfcv.ro; manuel.amzoiu@umfcv.ro.
[2] Danubius International University, Faculty of Behavioral and Applied Sciences, 8000654 Galati, Romania.
[3] University of Life Science "King Michael I", 300645 Timisoara, Romania. E-mail: sofiapopescu@usvt.ro
[4] University of Medicine and Pharmacy, Faculty of Medicine, 200349 Craiova, Romania.
E-mail: oana.taisescu@umfcv.ro.
* *Corresponding authors: adrianbeteringhe@univ-danubius.ro; mihaela.subtirelu@umfcv.ro.*

https://doi.org/10.46939/J.Sci.Arts-26.1-b02

Initially, the enzyme was studied for its role in regulating glycogen synthesis [3-5]. In recent years, however, studies have expanded as GSK-3 has been found to play an important role in many cellular processes, including insulin action, gene transcription, cell death and survival, cell differentiation, neuronal function, circadian rhythms, and the renewal and differentiation of stem cells [6]. GSK-3 is a multifunctional serine/threonine kinase found in all eukaryotes, playing a central role in the regulation of numerous cell signalling pathways [7,8].

Inhibition of the GSK-3 enzyme can help treat diseases such as diabetes [9], Alzheimer's disease [10], Huntington's disease [11], bipolar affective disorder, schizophrenia [12], head trauma, chronic inflammatory processes [13] and certain types of cancer [14,15].

For these reasons, studies aimed at discovering treatments for these diseases focus on developing new, potent, and selective GSK-3 inhibitors [16]. For this, the mechanism of inhibitor interaction with the GSK-3 enzyme must be known. A detailed understanding of the drug-receptor association process is fundamental to drug design.

Most pharmacological inhibitors of GSK-3 have the following properties in common: (i) they have a low molecular weight; (ii) they are hydrophobic heterocycles; (iii) most act in the ATP binding site of the kinase through hydrogen bonds [17,18].

The present study joins those seeking to shed light on this direction by identifying the binding mode of the inhibitory molecules to the GSK-3β enzyme. Thus, this paper aimed to identify the molecular fragments responsible for the inhibitory effect of aloisins on this enzyme. The identification of binding sites is very important for the design of new compounds with inhibitory activity against GSK-3β and, therefore, for the prevention and treatment of serious, incurable diseases. On the other hand, this research explores the structure-activity relationship of aloisines and elucidates their binding mechanisms through molecular docking. By examining how the structural variations in aloisines affect their inhibitory potency, we can gain insights into the key interactions that govern their efficacy. Molecular docking studies will further elucidate the binding affinity and orientation of aloisines within the GSK-3β active site, providing a comprehensive understanding of their inhibitory potential. This research not only advances the development of aloisines as potential GSK-3β inhibitors but also deepens our understanding of structure-based drug design for targeting this pivotal kinase.

2. MATERIALS AND METHODS

2.1. MATERIALS

The substances under study are aloisine derivatives (6-phenyl-5H-pyrrolo[2,3-b]pyrazine), a new family of dual GSK-3β/CDK inhibitors that have proven effective in the curative treatment of diseases involving the 2 enzymes.

The inhibitory activity values are reported in the literature [19] and are presented in Table 1. Biological activity is expressed as $pIC_{50} = -\log IC_{50}$, where IC_{50} represents the concentration for which a maximum biological response is obtained.

Table 1. Inhibitory activity of aloisine derivatives [19].

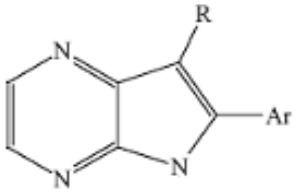

Cmpd	R	Ar	pIC_{50}	*Cmpd*	R	Ar	pIC_{50}
1	H	Phenyl	5.64	19	CH_3	4-dimethylamino sulfamoylphenyl	6.30
2	H	2-metoxyphenyl	5.48	20	$(CH_2)_2CH_3$	4-methoxyphenyl	6.40
3	H	2-hydroxyphenyl	5.19	21	$(CH_2)_2CH_3$	4-hydroxyphenyl	5.74
4	H	3-metoxyphenyl	5.50	22	CH_2-CH=CH_2	4-methoxyphenyl	6.22
5	H	4-metoxyphenyl	5.96	23	$(CH_2)_2CH_2Cl$	4-methoxyphenyl	5.60
6	H	4-hydroxyphenyl	5.92	24	$CH(CH_3)_2$	4-methoxyphenyl	6.30
7	H	3,5-dimetoxyphenyl	4.22	25	$CH(CH_3)_2$	4-chlorophenyl	6.12
8	H	3,4,5-trimetoxyphenyl	4.07	26	$(CH_2)_3CH_3$	4-methoxyphenyl	6.04
9	H	4-fluorophenyl	5.72	27	$(CH_2)_3CH_3$	4-hydroxyphenyl	6.19
10	H	4-bromophenyl	5.22	28	$(CH_2)_3CH_3$	4-chlorophenyl	5.23
11	H	4-triflouromethylphenyl	5.14	29	$(CH_2)_6CH_3$	4-methoxyphenyl	5.00
12	H	4-cyanophenyl	5.32	30	CH_2-C_3H_5	4-methoxyphenyl	5.96
13	H	4-methylphenyl	5.59	31	CH_2-C_3H_5	4-hydroxyphenyl	5.52
14	H	4-dimethylaminophenyl	4.92	32	CH_2-C_6H_5	H	6.00
15	CH_3	4-methoxyphenyl	6.34	33	CH_2-C_6H_5	4-chlorophenyl	5.17
16	CH_3	4-hydroxyphenyl	6.28	34	CH_2-C_6H_{11}	4-methoxyphenyl	5.17
17	CH_3	3,4-dimetoxyphenyl	5.70	35	CH_2-C_6H_{11}	4-chlorophenyl	5.10
18	CH_3	4-chlorophenyl	5.77				

2.2. METHODS

Our study is based on quantitative structure-activity relationships to gain structural insight into how molecules bind to GSK-3β and use the descriptors provided by dedicated programs, such as the CODESSA program (Comprehensive Descriptors for Structural and Statistical Analysis) [20,21] or "window" descriptors of the electronegativity type of the quantum molecular states of these bioactive compounds [22,23].

In this sense, molecular modelling and optimisation were performed using the program HyperChem 8.0 [24] and Molecular Mechanics (MM+) with Molecular Orbital Package (MOPAC). Semiempirical quantum molecular calculations were performed using the MOPAC 7 molecular quantum approximation (RHF, PM3) [25]. The atomic coordinates thus obtained were used as input data for the CODESSA program. This soft-pack calculates about 400 descriptors across a wide variety (topological, quantum-chemical, constitutional, geometric, or electrostatic), thus enabling a better investigation of drugcompound –biological receptor interactions.

3. RESULTS AND DISCUSSION

3.1. RESULTS

3.1.1. Chemical Characterization

The best Hansch correlation equations obtained with CODESSA [20,21] are listed in Table 2. They are of the form pIC50 = $a_0 + \Sigma_k a_k X_k$, where A is the biological activity, X_k are the structural descriptors (6, 5, 3 and 2 descriptors) and a_0, a_k are the coefficients by which the descriptors contribute to the formation of the biological activity.

Table 2. Linear Regression: pIC_{50} (experimental) = $a_0 + \Sigma_k a_k X_k$.

No. of correlated parameters (k)	*Correlation coefficient, R^2*	*F*	*Descriptors involved*	
6	0.8865	27.62	160 47 159 107 223 149	160 - Min (>0.1) bond order of a C atom 47 - HOMO energy 159 - Avg valency of a C atom 107 - RNCG Relative negative charge (QMNEG/QTMINUS) [Quantum-Chemical PC] 223 - Min n-n repulsion for a C-H bond 149 - Max bonding contribution of a MO 102 - FNSA-3 Fractional PNSA (PNSA-3/TMSA) [Quantum-Chemical PC] 63 - Avg electroph. react. index for a C atom 217 - Min exchange energy for a C-H bond 48 – HOMO-1 energy
	0.8539	25.05	160 47 102 63 217 149	
5	0.8260	25.73	160 47 159 107 223	
	0.8056	25.34	160 47 159 107 217	
3	0.7553	28.28	160 47 159	
	0.7476	25.00	160 47 102	
2	0.6454	27.78	160 48	
	0.6367	26.41	160 47	

One can observe that, in all the Hansch equations, the great variety of descriptors, most of them have to do with the "internal" formation of chemical bonds in each aloisine molecule studied (descriptors 160, 159, 223, 217, 149, 63). There is a large number of descriptors for C-H bonds or carbon atoms, which suggests the involvement of carbon atoms in the studied chemical structures in the formation of their biological activity.

The other descriptors relate to drug-receptor interactions (47, 48, 107, 102). These descriptors are called "external" descriptors and concern possible interactions between the drug and the atoms in the biological receptor's active site.

As shown in Table 2, the best-fit Hansch equation contains 6 descriptors, and the detailed results of the study are presented in Table 3.

Table 3. Linear Regression pIC_{50} [experimental] = $a_0 + \Sigma_k a_k X_k$ for k = 6 descriptors

Parameter	***Value***	***Error***	***t-test***
a_0 (intercept.)	$5.0605 \cdot 10^{+02}$	$8.9442 \cdot 10^{+01}$	5.6767
a_1 (160 descr. coef.)	$-1.8328 \cdot 10^{+00}$	$2.5816 \cdot 10^{-01}$	-7.4871
a_2 (47 descr. coef.)	$3.9047 \cdot 10^{+00}$	$5.0396 \cdot 10^{-01}$	7.7436
a_3 (159 descr. coef.)	$-1.0591 \cdot 10^{+02}$	$2.0240 \cdot 10^{+01}$	-5.2329
a_4 (107 descr. coef.)	$1.4787 \cdot 10^{+01}$	$3.1327 \cdot 10^{+00}$	4.7332
a_5 (223 descr. coef.)	$-1.7171 \cdot 10^{+00}$	$4.1906 \cdot 10^{-01}$	-4.0974
a_6 (149 descr. coef.)	$9.3237 \cdot 10^{+00}$	$3.3710 \cdot 10^{+00}$	2.7623
R^2	F	N	s^2
0.8865	27.62	35	0.0562

Based on the results in Table 3, pIC_{50} values for the inhibitory activity can be calculated. Mathematical estimation of pIC_{50} activity based on the regression equation $pIC_{50} = a_0 + \Sigma_k a_k X_k$ for k = 6 descriptors is presented in Table 4.

Table 4. Comparison of experimental and calculated pIC_{50} values.

Cmpd	***Predicted pIC_{50}***	***Exper. pIC_{50}***	***Residual pIC_{50}***	***Cmpd***	***Predicted pIC_{50}***	***Exper. pIC_{50}***	***Residual pIC_{50}***
1	5.7183	5.6400	0.0983	19	5.9100	5.9600	-0.0500
2	5.8926	5.4800	0.4006	20	5.0852	5.1700	-0.0848
3	5.3087	5.1900	0.1187	21	6.2140	6.3000	-0.0860
4	5.9478	5.9600	- 0.0222	22	5.8003	5.7700	0.0303
5	5.7531	5.9200	- 0.1669	23	6.0083	6.1200	-0.1117
6	4.2122	4.2200	- 0.0078	24	5.1998	5.2300	-0.0302
7	4.0792	4.0700	0.0092	25	5.1998	5.1700	0.0298
8	5.5615	5.7200	- 0.1685	26	5.4392	6.0000	-0.5608
9	5.5920	5.2200	0.3720	27	5.9674	6.2800	-0.3126
10	5.0696	5.1400	- 0.0704	28	5.9039	5.7400	0.1639
11	5.6306	5.5900	0.0406	29	5.7248	5.5200	0.2048
12	5.0430	5.3200	-0.2770	30	5.9575	6.1900	-0.2325
13	6.2013	6.3400	-0.1387	31	5.5141	5.5000	0.0141
14	5.6600	5.7000	-0.0400	32	6.0003	6.0400	-0.0397
15	5.9758	5.6000	0.3758	33	5.2611	4.9200	0.3411
16	6.5114	6.3000	0.2114	34	6.1359	6.4000	-0.2641
17	6.1170	6.2200	-0.1030	35	5.0852	5.1000	-0.0148
18	5.3706	5.0000	0.3706				

Fig. 1 shows that the predicted (calculated) pIC_{50} values correlate well with the actual values [19], indicating the predictive ability of the mathematical model.

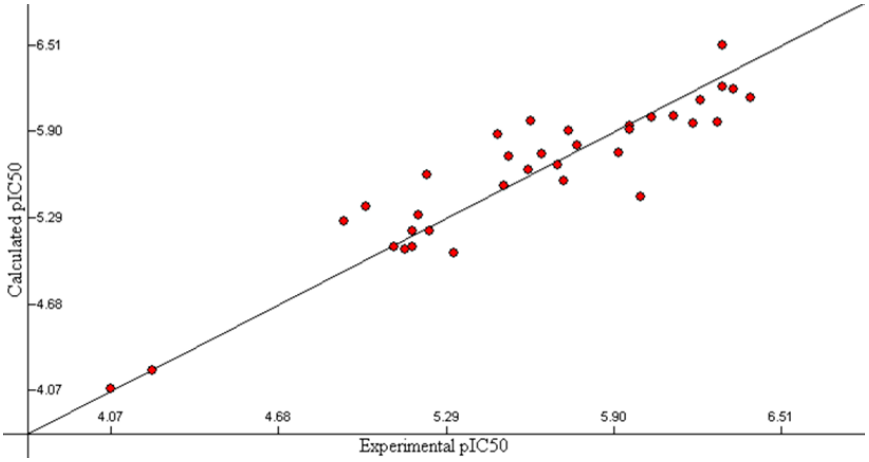

Figure 1. Predicted activity - experimental activity correlation for the Hansch equation $pIC_{50} = a_0 + \Sigma_k a_k X_k$, k = 6.

3.1.2. Analysis of Atomic Species Contributions to Inhibitory Activity using Electronegativity Fingerprint Descriptors

To determine the contribution and role of the atomic species in each molecule to the formation of the biological response, the inhibitory activity of the studied class of substances was analyzed using fingerprint descriptors, such as the electronegativity of the atoms in the molecule. These parameters must reflect the ability of the atoms in the molecule to transfer electron densities between the bioactive molecule and the biological receptor [22,23]. The electronegativity descriptor values are presented in Tables 5 and 6.

Table 5. HOMO electronegativity for atoms of the aloisines.

Cmpd	*HEL*	*HELH*	*HELC*	*HELO*	*HELN*	*HELX*	*Cmpd*	*HEL*	*HELH*	*HELC*	*HELO*	*HELN*	*HELX*
1	5.835	0.000	5.295	0.000	0.519	0.000	19	5.844	0.029	5.075	0.281	0.459	0.000
2	5.927	0.009	5.321	0.073	0.514	0.000	20	5.870	0.083	4.601	0.000	1.180	0.000
3	5.864	0.014	5.297	0.317	0.240	0.000	21	6.251	0.250	4.701	0.075	1.193	0.032
4	5.900	0.034	5.254	0.328	0.274	0.000	22	6.105	0.200	4.776	0.000	0.691	0.439
5	5.877	0.000	5.294	0.281	0.302	0.000	23	5.999	0.000	4.977	0.000	0.529	0.493
6	5.755	0.000	5.174	0.080	0.481	0.000	24	6.090	0.075	4.851	0.000	0.723	0.440
7	5.789	0.000	5.292	0.156	0.341	0.000	25	6.314	0.237	4.385	0.000	1.415	0.277
8	5.935	0.000	5.332	0.000	0.492	0.133	26	6.299	0.157	4.518	0.000	1.624	0.000
9	5.856	0.000	5.147	0.000	0.530	0.179	27	6.030	0.185	5.100	0.243	0.503	0.000
10	5.872	0.000	5.069	0.000	0.782	0.021	28	6.118	0.072	4.940	0.202	0.903	0.000
11	5.827	0.089	5.450	0.000	0.388	0.000	29	6.095	0.080	4.955	0.203	0.857	0.000
12	5.910	0.000	5.205	0.000	0.706	0.000	30	6.043	0.081	4.860	0.196	0.906	0.000
13	5.811	0.027	5.029	0.272	0.483	0.000	31	5.800	0.014	5.255	0.108	0.423	0.000
14	5.720	0.004	5.053	0.037	0.627	0.000	32	5.936	0.027	4.907	0.244	0.758	0.000
15	5.911	0.032	4.888	0.274	0.715	0.001	33	5.822	0.008	5.332	0.000	0.482	0.000
16	5.984	0.028	4.993	0.252	0.711	0.000	34	5.923	0.028	4.886	0.243	0.767	0.000
17	5.877	0.029	5.143	0.288	0.417	0.000	35	5.864	0.083	4.601	0.000	1.180	0.000
18	5.930	0.027	4.839	0.233	0.832	0.000							

EL - total electronegativity, ELH - electronegativity of hydrogen atoms, ELC - electronegativity of the carbon atom, ELN – the electronegativity of the nitrogen atom, ELO – the electronegativity of the oxygen atom, ELX - the electronegativity of the halogen atom; H prefix refers to the HOMO state

Table 6. LUMO electronegativity for atoms of the aloisines.

Cmpd	*LEL*	*LELH*	*LELC*	*LELO*	*LELN*	*LELX*	*Cmpd*	*LEL*	*LELH*	*LELC*	*LELO*	*LELN*	*LELX*
1	6.342	0.000	4.186	0.000	2.156	0.000	19	6.409	0.012	4.205	0.062	2.130	0.000
2	6.357	0.008	4.442	0.014	1.892	0.000	20	6.271	0.018	4.270	0.000	1.983	0.000
3	6.391	0.011	4.184	0.042	2.154	0.000	21	8.020	0.028	2.577	0.608	0.871	3.937
4	6.442	0.007	4.205	0.064	2.167	0.000	22	6.313	0.058	4.366	0.000	1.831	0.059
5	6.446	0.000	4.223	0.066	2.157	0.000	23	6.294	0.000	4.398	0.000	1.838	0.059
6	6.323	0.000	4.115	0.019	2.189	0.000	24	6.303	0.027	4.396	0.000	1.822	0.058
7	6.366	0.000	4.305	0.029	2.032	0.000	25	6.314	0.043	4.377	0.000	1.834	0.060
8	6.429	0.000	4.516	0.000	1.849	0.064	26	6.368	0.025	4.099	0.000	2.244	0.000
9	6.309	0.000	4.408	0.000	1.878	0.023	27	6.453	0.053	4.213	0.067	2.120	0.000
10	6.268	0.000	4.750	0.000	1.444	0.074	28	6.469	0.020	4.050	0.058	2.341	0.000
11	6.354	0.050	4.201	0.000	2.103	0.000	29	6.472	0.020	4.046	0.058	2.349	0.000
12	6.374	0.000	4.775	0.000	1.599	0.000	30	6.461	0.018	4.023	0.057	2.363	0.000
13	6.396	0.007	4.187	0.062	2.140	0.000	31	6.335	0.001	4.126	0.006	2.202	0.000
14	6.339	0.004	4.300	0.007	2.028	0.000	32	6.438	0.011	4.044	0.054	2.330	0.000
15	6.446	0.008	3.928	0.049	2.461	0.000	33	6.343	0.004	4.280	0.000	2.059	0.000
16	6.450	0.010	4.080	0.056	2.304	0.000	34	6.443	0.010	4.021	0.053	2.358	0.000
17	6.409	0.007	4.230	0.063	2.109	0.000	35	6.271	0.018	4.270	0.000	1.983	0.000
18	6.443	0.009	3.999	0.053	2.382	0.000							

EL - total electronegativity, ELH - electronegativity of hydrogen atoms, ELC - electronegativity of the carbon atom, ELN – the electronegativity of the nitrogen atom, ELO – the electronegativity of the oxygen atom, ELX - the electronegativity of the halogen atom; L prefix refers to the LUMO state

The statistical correlation between these descriptors and the biological activity yields correlation coefficients (R^2, %) for the component atoms of bioactive molecules (Table 7).

Table 7. Correlation coefficients R^2(%) for the electronegativity of molecular states.

Atom	HOMO	LUMO
H	5.80	4.52
C	1.85	**10.2**
O	**13.45**	**10.27**
N	0.42	0.43
X	0.00	4.53

3.1.3. Contribution of Oxygen and Carbon Atoms to HOMO/LUMO States in Biological Activity

As can be seen in Table 7, among the species of atoms in the studied molecules that contribute more to the formation of quantomolecular states, oxygen atoms stand out, their contribution to the formation of the HOMO state being 13.45% (HEO) and 10.27% for the formation of the LUMO state (LEO). Carbon atoms with a contribution of 10.2% (LEC) for the HOMO/LUMO states in the formation of the biological response are also noted. This is very likely because the HOMO and LUMO states are usually the most reactive in a molecule.

The values of the correlation coefficient suggest the possibility of an electron transfer between the oxygen and carbon atoms of the bioactive molecules (aloisine) and the atoms of the active site of the biological receptor, obviously followed by the formation of chemical bonds; oxygen atoms are electron donors and acceptors, and carbon atoms are only electron acceptors (Fig. 2).

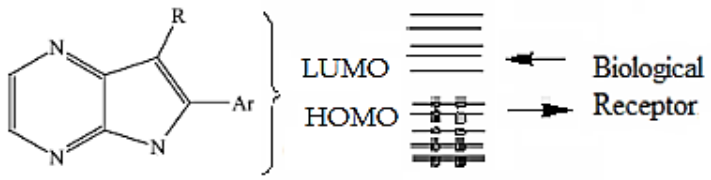

Figure 2. Ligand (aloisine) – biological receptor (GSK-3β) interaction.

An in-depth study can allow the identification of the atoms in the molecules that actually participate in the electronegativity of the analyzed molecular states. Thus, for one compound of the series (compound 2 from Table 1), the contributions of carbon atoms to the formation of the LUMO molecular state can be found by analyzing the *.mno output file obtained from Molecular Orbital PACkage (MOPAC) quantum chemical calculations. For this compound, the LUMO state is described by the molecular orbital no. 43.

For this molecular orbital, the contributions of the 28 atoms in the compound (Fig. 3) are summarized in Table 8 (the sum of the contributions of all atoms is equal to unity). The results indicate increased contributions of carbon atoms numbered 1, 5, 7 and 15 to the electronegativity of the LUMO state.

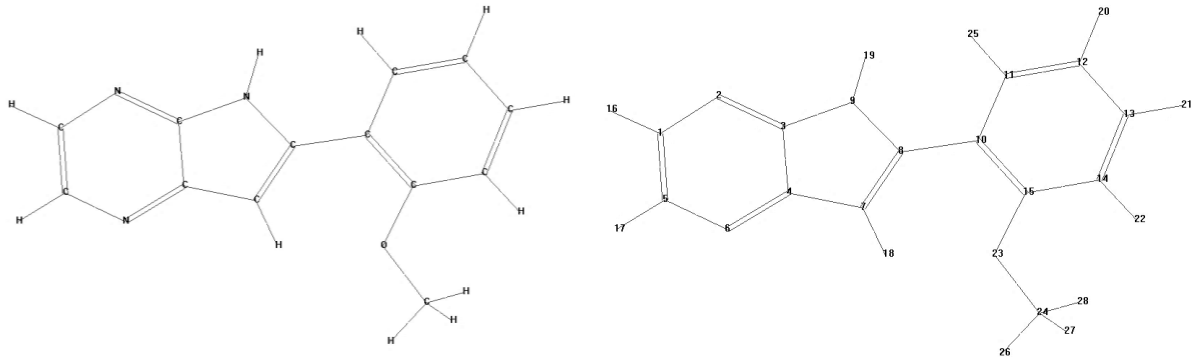

Figure 3. Compound 2 (Table 1) and numbering of component atoms.

Table 8. The contributions of atoms at the LUMO molecular state (MO no. 43) for compound 2.

1 C	**0.11271**	8 C	0.09652	**15 C**	**0.11390**	22 H	0.00000
2 N	0.09837	9 N	0.08229	16 H	0.00000	23 O	0.00224
3 C	0.00244	10 C	0.00922	17 H	0.00000	24 C	0.00343
4 C	0.06526	11 C	0.01552	18 H	0.00000	25 H	0.00001
5 C	0.**10684**	12 C	0.01938	19 H	0.00000	26 H	0.00000
6 N	0.08847	13 C	0.00711	20 H	0.00071	27 H	0.00011
7 C	**0.11271**	14 C	0.06258	21 H	0.00002	28 H	0.00016

These results are consistent with those mentioned above. Also, for most of the compound's nitrogen atoms (numbered 2 and 9) are involved in the interaction with the receptor.

3.1.4. Molecular docking

Fig. 4 shows the 2D interactions between some randomly chosen chemical compounds and GSK-3β enzyme (PDB number 1Q4L, collected from RCSB Protein Data Bank (PDB) [26]). The figure also shows the total interaction energies found using the HEX 8.0 docking program [27].

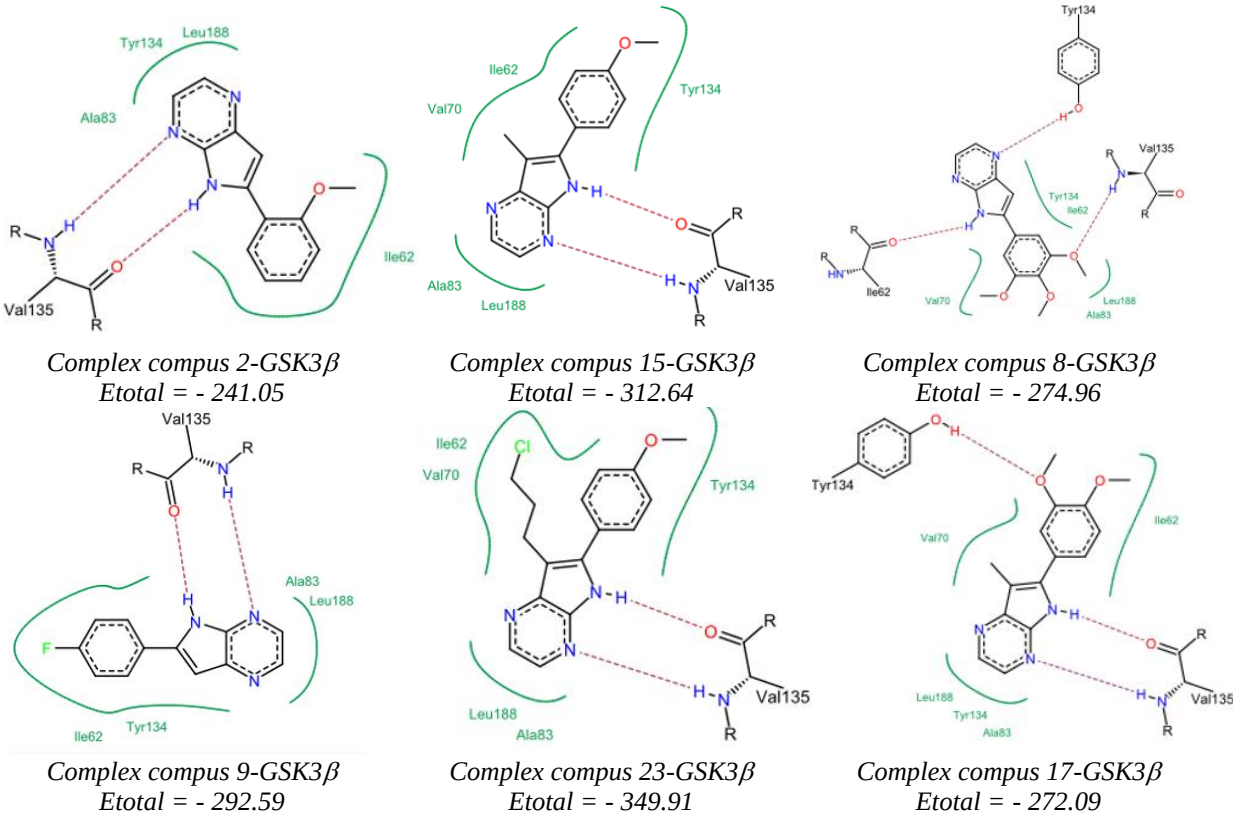

Complex compus 2-GSK3β
Etotal = - 241.05

Complex compus 15-GSK3β
Etotal = - 312.64

Complex compus 8-GSK3β
Etotal = - 274.96

Complex compus 9-GSK3β
Etotal = - 292.59

Complex compus 23-GSK3β
Etotal = - 349.91

Complex compus 17-GSK3β
Etotal = - 272.09

Figure 4. 2D interaction diagrams between chemical compounds and amino acids of the kinase binding site.

Molecular docking studies performed for all 35 bioactive compounds indicate the same docking region: in the vast majority of cases, the ligands bind to the same amino acid residues in the kinase active site (Leu188, Ala83, Tyr134, Ile62, Val110, Val70) through a variety of bonds. This fact can explain the relatively low differences between the inhibitory activity values of the analyzed molecules, pIC50 = 4.22 ÷ 6.40. Noteworthy is the presence of

C_1 and C_5 atoms from bioactive molecules in the Leu188, Ala83 amino acid area. This interaction is consistent with the results of the correlation study between pIC_{50} activity and the fingerprint descriptors, indicating that these atoms are involved in the interaction via the LUMO molecular state. Also, the involvement of the oxygen atom of the Ar group (3-methoxyphenyl) in compound 8 indicates its role as an acceptor via hydrogen bonding. Oxygen also participates in the interaction through donor hydrogen bonds in bioactive molecules, in which the Ar residue is a hydroxyphenyl group.

These observations allow us to identify regions of the bioactive aloisine molecule that underlie its characteristic biological activity (Fig. 5).

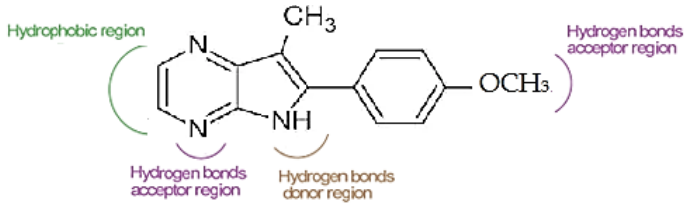

Figure 5. Molecular active sites for the 15-numbered aloisine derivative.

3.2. DISCUSSION

The investigation into the inhibitory activity of aloisines on GSK-3β has yielded significant insights into the structure-activity relationships and molecular interactions that underlie their potential as therapeutic agents. The structure-activity correlation analysis revealed that specific functional groups and structural motifs within aloisines are critical for their binding affinity and inhibitory potency. For instance, hydroxyl groups and other polar substituents enhance hydrogen bonding with key residues in the GSK-3β active site, thereby increasing the inhibitory efficacy. Conversely, non-polar groups and bulky substituents may hinder optimal binding by causing steric clashes or reducing favorable interactions.

Studies conducted to date on enzyme inhibitors suggest that the vast majority act by competitively inhibiting ATP binding to the kinase's catalytic subunit [28,29]. Aloisines also interact with the ATP-binding pocket through two hydrogen bonds with the nitrogen and oxygen atoms of Leu 83 [30].

In the following, we discuss our perspective on the interaction of aloisine molecules with the GSK-3β receptor. Between these two types of descriptors, there is a link (hierarchy) [31], which allows a better choice of those statistical equations that can be used in the optimization and design of molecular structures with predictable activity.

It can also be observed in the studied case of the Hansch equations, with 6 descriptors, that the internal descriptors appear as a kind of "background noise" in all statistical equations, although their presence is not justified by the principles of physicochemical ligand-receptor interaction. This can only be explained by the link between the two types of descriptors. Thus, the external molecular shape descriptors depend on the spatial arrangement of the atoms, which is influenced by many other factors that condition the internal descriptors, such as the nature of the atoms, the formation of chemical bonds, the stabilization energy of the molecular system, etc. Also, descriptor 107, based on the distribution of electric charges on the atoms in the molecule, depends on the internal descriptors that determine the partitioning of the electronic population within the molecule.

Molecular docking studies further corroborated these findings by demonstrating the precise binding orientations of aloisines within the GSK-3β active site. The docking simulations highlighted that effective inhibitors consistently form strong hydrogen bonds with

the ATP-binding pocket residues and engage in hydrophobic interactions that stabilize the inhibitor-enzyme complex. Notably, aloisines with enhanced inhibitory profiles exhibited higher binding affinities, as evidenced by lower binding energy scores in the docking studies.

The importance of electronegativity descriptors of OMO/UMO quantum states has been indicated in several papers published under the coordination of Professor C.I. Lepădatu [22,23]. Their evaluation is performed on the output files of the MOPAC 2007 package [25] using an in-house program named Elwindow.

Such an analysis of the contributions of the atomic species and their locations opens a new avenue for identifying the molecular fragments that most contribute to the formation of biological activity [32]. This enables the design of new chemical structures with optimized bioactivity more easily.

The interactions between the active compounds and the amino acids at the target protein's binding site, as shown by QSAR analysis, are also supported by molecular docking studies performed with the FlexX program [33]. This technique allows visualization of the ligand (drug) - biological receptor interaction and predicts the optimized conformation of the stable complex formed by the interaction [34-36]. The bonds formed between the two participants in the interaction involve the oxygen atoms (grafted onto the phenyl residue) and the carbon atoms of the ligand molecules (aloisine derivatives).

The comprehensive analysis underscores the importance of fine-tuning the chemical structure of aloisines to maximize their inhibitory potential. The correlation between structural features and biological activity not only aids in the rational design of more potent GSK-3β inhibitors but also provides a framework for developing novel therapeutic strategies targeting GSK-3β-related pathologies. Future studies should focus on synthesizing and testing derivatives with optimized functional groups to validate the predicted interactions and to further refine the structure-activity relationship models. Overall, the integration of structure-activity correlation and molecular docking studies presents a robust approach for advancing the development of aloisines as promising GSK-3β inhibitors.

4. CONCLUSIONS

From QSAR studies conducted on a class of aloisines considered GSK-3β inhibitors, new results were obtained regarding the mechanism of interaction between the ligand and the receptor, the nature of these interactions, and the possibility of identifying the active molecular fragments. Thus, using the descriptors implemented in the CODESSA program, correlation equations were obtained linking the inhibitory activity of the aloisine derivatives to their structure. Among the descriptors present in these equations, it can identify descriptors that address the "internal" formation of C-H chemical bonds in each studied molecule, suggesting the involvement of carbon atoms in the biological response. In addition to these descriptors, the correlation equations include descriptors such as the electric charges of atoms in the chemical structures, which indicate the predominance of electrostatic interactions between the ligand (aloisine derivative) and the biological receptor (GSK-3β). The QSAR study using the electronegativity descriptors of occupied or unoccupied molecular states with electrons in the molecule highlighted the involvement of oxygen atoms, 13.45% and 10.27%, respectively, for the HOMO/LUMO states in the formation of the biological response. In the HOMO and LUMO states, which are the most reactive states of a molecule, carbon atoms participate with 10.2% in the LUMO state in the formation of biological activity.

The analysis of the contributions of atom species and their locations opens a new way to identify the molecular fragments or chemical groups that contribute most to drug activity.

The identification of such active parts in chemical structures enables the design of new chemical structures with optimized, predictable inhibitory drug activity.

The interactions between the active compound (aloisine) and the amino acids at the binding site of the target protein (GSK-3), as revealed by QSAR analysis, are also supported by molecular docking studies.

Acknowledgements: *We would like to dedicate this article to the memory of Professor Costinel Lepădatu.*

REFERENCES

[1] Embi, N., Rylatt, D. B., Cohen, P., *Eur. J. Biochem.*, **107**(2), 519-527, 1980.
[2] Welsh, G. I., Proud, C. G., *Biochem. J.*, **15**, 625-629, 1993.
[3] Frame, S., Cohen, P., *Biochem. J.*, **359**, 1-16, 2001.
[4] Doble, B. W., Woodgett, J. R., *J. Cell Sci.*, **116**, 1175-1186, 2003.
[5] Jope, R. S., Johnson, G. V. W., *Trends Biochem. Sci.*, **29**, 95-102, 2004.
[6] Piazzi, M., Bavelloni, A., Cenni, V., Faenza, I., Blalock, W. L., *Cells*, **10**(11), 3255, 2021.
[7] Cohen, P., *Nat. Rev. Drug Discov.*, **1**, 309-315, 2002.
[8] Noble, M. E., Endicott, J. A., Johnson, L. N., *Science*, **303**(5665), 1800-1805, 2004.
[9] Gokhale, K.M., Tilak, B.P., *Int. J. Pharm. Phytopharmacol. Res.*, **3**, 196-199, 2013.
[10] Cai, Z., Zhao, Y., Zhao, B., *Int. J. Mol. Sci.*, **9**, 864-879, 2012.
[11] Lim, N. K. H., Hung, L. W., Pang, T. Y., Mclean, C. A., Liddel, J. R., Hilton, J. B., Li, Q. X., White, A. R., Hannan, A. J., Crouch, P. J., *Hum. Mol. Genet.*, **23**, 4051-4063, 2014.
[12] Jope, R. S., Roh, M. S., *Curr. Drug Targets*, **7**, 1421-1434, 2006.
[13] Jope, R. S., Yuskaitis, C. J., Beurel, E., *Neurochem. Res.*, **32**, 577-595, 2007.
[14] Mancinelli, R., Carpino, G., Petrungaro, S., Mammola, C. L., Tomaipitinca, L., Filippini, A., Facchiano, A., Ziparo, E., Giampietri, C., *Oxid. Med. Cell. Longev.*, **2017(1)**, 4629495, 2017.
[15] Zhang, M., Zhang, L., Hei, R., Li, X., Cai, H., Wu, X., Zheng, Q., Cai, C., *Am. J. Cancer Res.*, **11**, 1913-1935, 2021
[16] Xu, M., Wang, S. L., Zhu, L., Wu, P. Y., Dai, W. B., Rakesh, K. P., *Eur. J. Med. Chem.*, **164**, 448-470, 2019.
[17] Pandey, M. K., DeGrado, T. R., *Theranostics*, **6**, 571-593, 2016.
[18] Meijer, L., Flajolet, M., Greengard, P., *Trends Pharmacol. Sci.*, **25**, 471-480, 2004.
[19] Zeng, M., Jiang, Y., Zhang, B., Zheng, K., Zhang, N., Yu, Q., *Bioorg. Med. Chem. Lett.*, **15**, 395-399, 2005.
[20] Schmidt, M. W., Bridge, K. K., Boatz, J. A., Elrbert, S. T., Gordon, M. S., Jensen, J. H., Koseki, S., Matsunaga, N., Nguyen, K. A., Su, S., Windus, T. L., Dupuis, M., Montgomery Jr, J. A., *J. Comput. Chem.*, **14**, 1347-1363, 1993.
[21] Katritzky, A. R., Petrukhin, R., Yang, H., Karelson, M., CODESSA PRO User's Manual, University of Florida, Gainesville, FL, USA: 2002. https://www.codessa-pro.com/manuals/CODPROUS.pdf (accessed on December 15th, 2025)
[22] Amzoiu, E., Anoaica, P. G., LepAdatu, C. I., *Rev. Roum. Chim.*, **56**, 711-716, 2011.
[23] LepAdatu, C. I., Culita, D. C., Patron, L., *Optoelectron. Adv. Mat. - Rapid Comm.*, **4**, 160-164, 2010.

[24] http://www.hypercubeusa.com/
[25] MOPAC 2007, JJP Stewart, Stewart Computational Chemistry, Colorado Springs, CO, USA, http://openMOPAC.net 2007.
[26] http://www.rcsb.org/
[27] Macindoe, G., Mavridis, L., Venkatraman, V., Devignes, M. D., Ritchie, D. W., *Nucleic Acids Res.*, **38**(2), W445-W449, 2010.
[28] Coghlan, M.P., Culbert, A. A., Cross, D. A. E., Corcoran, S. L., Yates, J. W., Pearce, N. J., Rausch, O. L., Murphy, G. J., Carter, P. S., Cox, L. R., Mills, D., Brown, M., Haigh, D., Ward, R. W., Smith, D. G., Murray, K. J., Reith, A. D., Holder, J. C., *Chem. Biol.*, **7**(10), 793-803, 2000.
[29] Eldar-Finkelman, H., Martinez, A., *Front. Mol. Neurosci.*, **4**, 32, 2011.
[30] Mettey, Y., Gompel, M., Thomas, V., Garnier, M., Leost, M., Ceballos-Picot, I., Noble, M., Endicott, J., Vierfond, J. M., Meijer, L., *J. Med. Chem.*, **46**, 222-236, 2003.
[31] Anoaica, P. G., Amzoiu, E., Lepădatu, C.I., *Rev. Roum. Chim.*, **52**, 789-793, 2007.
[32] Amzoiu, M., Amzoiu, E., Belu, I., Popescu, S., Cheita, G., Amzoiu, D., *Journal of Science and Arts*, **19**(2), 469-478, 2019.
[33] Rarey, M., Kramer, B., Lengauer, T., Klebe, G., *J. Mol. Biol.*, **261**, 470-489, 1996.
[34] Amzoiu, M.O., Popescu, G. S., Amzoiu, E., Ciocilteu, M. V., Manda, C. V., Rau, G., Gresita, A., Taisescu, O., *Life*, **15**(8), 1247, 2025.
[35] Amzoiu, M.O., Taisescu, O., Amzoiu, E., Gresita, A., Popescu, G. S., Rău, G., Ciocilteu, M. V., Manda, C. V., *Life*, **15**(12), 1903, 2025.
[36] Viezuin, A, D. M., Burlacu (Mușa), I., Gresita, A., Matache, I. M., Tartea, E. A., Musat, M. I., Amzoiu, M. O., Catalin, B., Sfredel, V., Mitran, S., *Int. J. Mol. Sci.*, **27**(1), 419, 2026.